Charge storage mechanism of manganese dioxide for capacitor application: Effect of the mild electrolytes containing alkaline and alkaline-earth metal cations

Chengjun Xu[a], Chunguang Wei[a,b], Baohua Li[a], Feiyu Kang[a,b,*], Zhicheng Guan[c]

[a] *Advanced Materials Institute, Graduate School at Shenzhen, Tsinghua University, Shenzhen City, Guangdong Province, 518055, China*
[b] *Laboratory of Advanced Materials, Department of Materials Science and Engineering, Tsinghua University, Beijing, 100084, China*
[c] *Graduate School at Shenzhen, Tsinghua University, Shenzhen City, Guangdong Province, 518055, China*

ABSTRACT

Effect of the electrolyte particularities on manganese dioxide in the neutral electrolytes containing alkaline (Li^+, Na^+, or K^+) and alkaline-earth (Mg^{2+}, Ca^{2+}, or Ba^{2+}) metal cations for electrochemical capacitor is investigated by cyclic voltammetry and electrochemical impedance spectroscopy. A very high capacitance of 357.9 F g^{-1} is measured when Ca^{2+} ion is used as electrolyte cation. The results show that cations of the electrolyte instead of proton or anions are responsible for the pseudo-capacitive behavior of manganese dioxide. The capacitance of manganese dioxide is found to depend strongly on the electrolyte particularities, for example, pH value, cation and anion species, and salt concentrations. A logarithmic dependence of capacitance of MnO_2 on cation activity is obtained for all alkaline and alkaline-earth metal cations. The capacitance of MnO_2 can be doubled by replacing univalent cation with bivalent cation at a close cation activity.

© 2011 Elsevier B.V. All rights reserved.

1. Introduction

Electrochemical capacitors or supercapacitors are now widely used for various applications from consumer electronics, electric vehicles, satellites, to military applications [1,2]. Based on charge storage mechanism, supercapacitors can be categorized into electric double-layer capacitors (EDLCs) and pseudocapacitors. Carbon materials with a large specific surface area are widely used in the EDLCs, while a series of metal oxides exhibiting a pseudo-capacitive behavior use nontoxic and nonflammable aqueous electrolytes [1]. RuO_2 is a well-known electrode material with the pseudo-capacitive behavior due to its high capacitance. However, its high cost prevents it from a large scale application [1]. In recent years, researchers have paid more attentions to low cost and environmentally friendly alternative materials, such as, manganese oxides, vanadium oxides, and iron oxides [3–5]. Among them, manganese dioxide has been considered as the most promising one due to its low cost, non-toxicity, and abundance in raw materials. The increasing worldwide interest in MnO_2 for supercapacitor appli-

cations is based on anticipation that MnO_2 supercapacitors will ultimately serve as safety and low cost alternative to current commercial organic EDLCs and RuO_2-based acid systems [3].

The so-called amorphous alpha manganese dioxide (MnO_2) generally shows the capacitive behavior in the mild electrolytes containing alkaline metal cations with an infinite cycle life [3–7]. The electrochemical performance of MnO_2 is determined by its physicochemical properties, for example, specific surface area, crystalline geometry, water content, surface chemistry, etc. and the electrolyte particularities such as cation species and concentration. Until now, the researches on the charge storage mechanism of MnO_2 in the mild electrolytes generally limit to the influence of physicochemical properties of MnO_2 [8–19]. For example, the effects of tunnel structure and water content of MnO_2 have been discussed in detail [8,17–19]. Since the whole charge storage process involves both MnO_2 itself and the electrolyte, the researches should not focus only on the physicochemical properties of MnO_2. But the effect of the electrolyte has to be understood in detail. Although a few papers has explored the influence of cation concentration and found a logarithmic dependence of capacitance on alkaline metal cation activity [20,21], however, the influence of electrolyte particularities is not yet further investigated. In addition, more recently, we have proposed a multivalent charge storage mechanism of MnO_2 and found that by replacing univalent cation with bivalent cation, for example, replacing conventional Na^+ ion with Ca^{2+} ion, a significant improvement (close to 80%) on the spe-

Table 1
Information of alkaline and the alkaline-earth metal cations.

Ion species	Ion size (Å)	Hydrated ion size (Å)	Standard redox potential (V)
Li^+	0.69	6	−3.05
Na^+	1.02	4	−2.71
K^+	1.38	3	−2.93
Mg^{2+}	0.66	8	−2.38
Ca^{2+}	0.99	5	−2.84
Ba^{2+}	1.34	6	−2.92

cific capacitance of the MnO_2 electrodes has been obtained [22,7]. However, the mechanism of capacitance enhancement is not clear. Therefore, the role of the electrolyte as well as the capacitance enhancement mechanism is necessary to be fully understood.

Our work aims at obtaining a fully understanding of the role of the electrolytes, which contains alkaline (Li^+, Na^+, or K^+) or alkaline-earth (Mg^{2+}, Ca^{2+}, or Ba^{2+}) metal cations. The features of these cations are shown in Table 1 [23]. The role of electrolyte particularities, such as, cation species, salt concentrations, anions, and protons, will be discussed in detail. In addition, we also anticipate that this work could stand out the significance of the effect of the electrolyte on the metal oxides for supercapacitor applications.

2. Experimental

MnO_2 powder was synthesized by a one step microemulsion. The detailed information on the sample can be seen in Ref. [24]. The as-prepared sample is standard amorphous α-MnO_2 in a spherical shape with ~4 nm in diameter. In this paper, this sample is denoted as MnO_2 [24].

Electrodes were prepared by mixing 70 wt% of MnO_2 powder as an active material with 20 wt% acetylene black and 10 wt% poly-tetrafluoroethylene (PTFE). 70 mg of MnO_2 powder and 20 mg of acetylene black were first mixed and dispersed in ethanol by ultrasound mixing for 30 min. Then the ink was dried at 80 °C for 4 h to get dark mixed powder and 10 mg of PTFE was added to get a paste by adding a little of 1-methy-2-pyrrolidinone (NMP), which was cold rolled into thick films. Pieces of film with 3 mg weight, typically 1 cm² in size, were then hot-pressed at 80 °C under 100 MPa on a titanium plate.

Electrochemical tests were performed with an Im6e (Zahner) electrochemical station and all electrochemical measurements of MnO_2 electrodes were performed at 25 ± 1 °C. A piece of platinum gauze and saturated calomel electrode (SCE) were assembled as counter and reference electrodes. A luggin capillary faced the working electrode at a distant of 2 mm was used to minimize errors due to iR drop in the electrolyte. The cyclic voltammetric (CV) experiment was applied to MnO_2 in the mild electrolyte containing the alkaline (Li^+, Na^+, or K^+) and alkaline-earth (Mg^{2+}, Ca^{2+}, or Ba^{2+}) metal cations with a fixed sweep rate of 2 mV s⁻¹ due to the same charge or discharge time. The potential has been controlled between −0.1 to 0.9 V versus SCE. The specific capacitance (C) of MnO_2 can be estimated using half the integrated area of the CV curve to obtain the charge (Q), and subsequently being divided the charge by the mass of the active material (m) and the width of the potential window (ΔV):

$$C = \frac{Q}{\Delta V m} \qquad (1)$$

The electrochemical impedance spectroscopy (EIS) was conducted at 0.5 V versus SCE by sweeping frequencies from 10 mHz to 10 kHz. The measured impendence data were analyzed by using Zview software. The diffusion coefficient was calculated based on the radius ~2 nm of MnO_2 particle and the expression of the Warburg impendence.
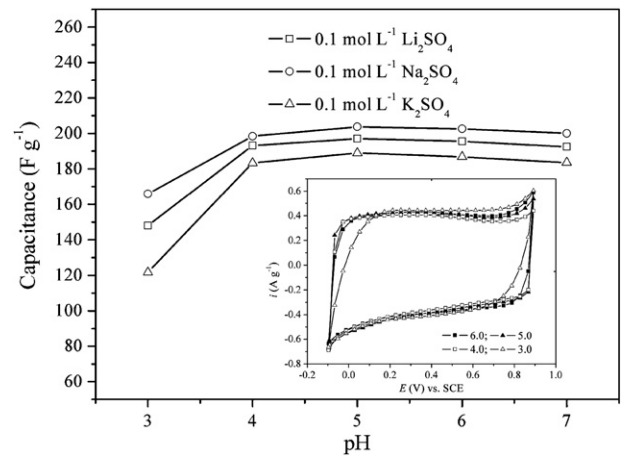

Fig. 1. Dependence of capacitance on the pH values in Li_2SO_4, Na_2SO_4, and K_2SO_4. Insert shows the cycle voltammetry plots of MnO_2 in 0.1 mol L⁻¹ Li_2SO_4 electrolyte with different pH values.

3. Results and discussion

3.1. Effect of proton

The electrolyte particularities only involve cation species, salt concentration, anion, and pH value (proton). Since the proton is usually considered as a crucial factor governing the charge storage process of MnO_2, we firstly investigate the effect of the proton by controlling the pH value (proton concentration) of 0.1 M Li_2SO_4, Na_2SO_4, and K_2SO_4 electrolytes. In order to investigate the role of proton, the pH value of all electrolytes has been controlled within 3–7 by adding H_2SO_4. Fig. 1 shows dependence of capacitance of MnO_2 on the pH value of the electrolytes. The insert picture shows the CV plots of MnO_2 in 0.1 M Li_2SO_4 electrolyte with different pH values. It can be seen that there is slight difference on capacitance and CV plots of MnO_2 which remain rectangular when pH value locates between 4 and 7. As pH value decreases to 3.0, the capacitance deceases sharply and the CV plot is less rectangular. The same phenomena have been discovered due to the dissolution of manganese from electrode to the electrolyte [25]. The constant capacitance and rectangular CV plots may indicate that proton is not involved in the charge storage process of MnO_2 in the neutral conditions (pH value locates between 4 and 7).
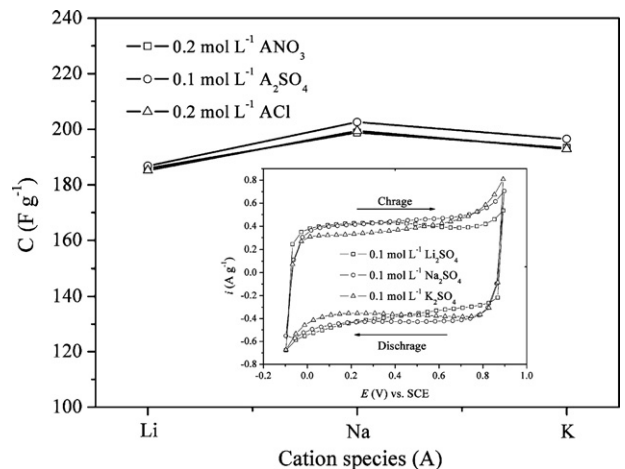

Fig. 2. The capacitance of MnO_2 in 0.2 M ANO_3, 0.1 M A_2SO_4 and 0.2 M ACl (pH value = 6.0), where A is alkaline metal cations (Li^+, Na^+, or K^+).
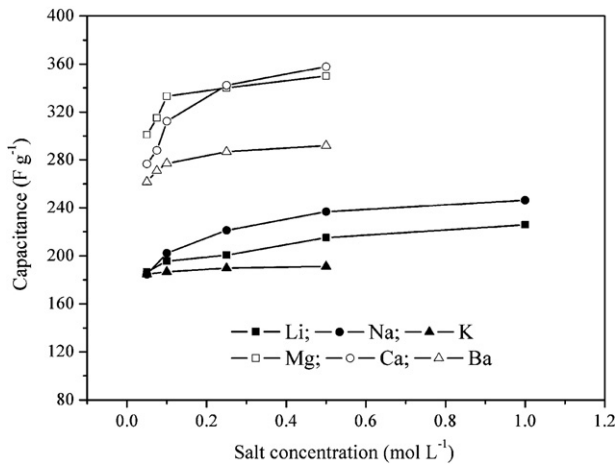
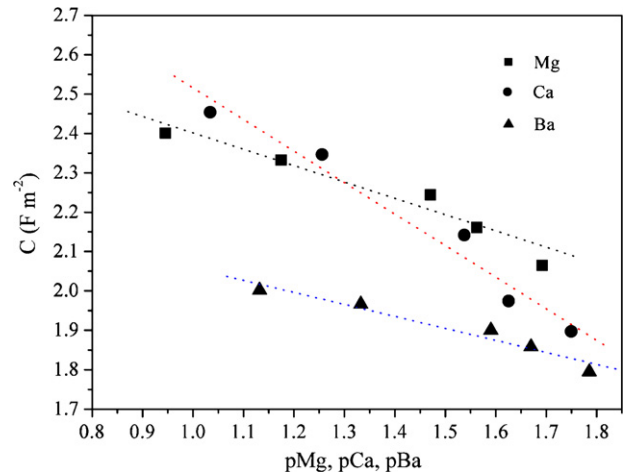**Fig. 3.** Dependence of capacitance on the salt concentration.

Fig. 4. Dependence of capacitance on pMg, pCa and pBa.

3.2. Effect of the anions

In order to investigate the effect of anions, we choose various anions (Cl^-, NO_3^- and SO_4^{2-}) with a fixed cation concentration (0.2 M). The capacitance of MnO_2 in 0.2 M ANO_3, 0.1 M A_2SO_4 and 0.2 M ACl (pH value = 6.0) is shown in Fig. 2, where A is alkaline metal cations (Li^+, Na^+, or K^+). It is seen that when the cation species is fixed the capacitance of MnO_2 are nearly constant for all anion species, which indicates that MnO_2 is inactive to the anions in the neutral electrolytes.

3.3. Effect of cation concentration (activity)

The researches on the proton and the anions indicate that the charge storage process of MnO_2 only involves the electrolyte alkaline or alkaline-earth metal cations and can be described as:

$$MnO_2 + xA^+ + xe^- \leftrightarrow A_xMnO_2 \tag{2}$$

where A^+ is the alkaline or alkaline-earth metal cation [4,9,14–17].

Therefore, the electrochemical performance of MnO_2 is only determined by the cation species with various ion sizes and hydrated ion sizes and cation concentration. To investigate the effect of cation species and concentration, we monitor the effect of cation species and concentration by using the alkaline and alkaline-earth metal cations as the ion probe.

The electrochemical performance of MnO_2 is investigated by CV and EIS in Li_2SO_4, Na_2SO_4, K_2SO_4, $Mg(NO_3)_2$, $Ca(NO_3)_2$, and $Ba(NO_3)_2$ electrolytes with various salt concentrations. Fig. 3 shows dependence of capacitance of MnO_2 on the cation concentration, which is determined from CV measurements. For all electrolytes, the specific capacitance increases as the cation concentration increases.

Considering the charge–discharge reaction of MnO_2 electrode in electrolytes (Eq. (2)), the rate law for charge–discharge step as an elementary reaction could be written as:

$$\text{Charge rate} = \frac{dq}{dt} = ka \tag{3}$$

where q is the charge, t is time, k is the charge rate constant, and a is cation activity [20,21]. The charge rate should be equal to the cation adsorption rate (da/dt) for the charge neutrality of the charge reaction. Hence the charge–discharge rate can be written as:

$$\frac{dq}{dt} = \frac{da}{dt} = ka \tag{4}$$

The differential equation $da/dt = ka$, thus has the solution: $\ln a = kt$. For the charge or discharge process of an electrochemical capacitor, the rate of charge of q with an arbitrary sweep rate (v) is given by $dq/dt = v\,dC/dt$ [20,21]. Hence, C is expected to show the logarithmic dependence on the cation activity, i.e. pA ($-\log a_A$).

The cation activity (a) can be written as:

$$a = f_i c \tag{5}$$

where a is ion activity, f_i is activity coefficient, and c is ion concentration. Activity coefficient (f_i) can be calculated according to Debye–Hückel equation:

$$-\log f_i = \frac{Az_i^2 I^{1/2}}{1 + B\mathring{a}I^{1/2}} \tag{6}$$

where f_i is activity coefficient, I is ionic strength, z_i is ion charge, A and B are coefficient, and $\mathring{a}$ is hydrated ion size of the cation (seen in Table 1). At 25 °C in aqueous solutions, A and B are 0.5115 and 0.3291, respectively [23]. Ionic strength (I) can be calculated from equation:

$$I = 0.5(c_+ z_+ + c_- z_-) \tag{7}$$

where c_+ and c_- are the concentration of cation and anion, and z_+ and z_- are the charge of cation and anion, respectively [23].

Table 2
The ionic strength, activity coefficient, and cation activity of the electrolytes containing alkaline-earth metal cations.

Salt concentration (mol L^{-1})		0.50	0.25	0.10	0.08	0.05
Ionic strength (I)		1.50	0.75	0.30	0.23	0.15
Cation concentration (mol L^{-1})		0.50	0.25	0.10	0.08	0.05
f_i	Mg^{2+}	0.23	0.27	0.34	0.37	0.41
	Ca^{2+}	0.19	0.22	0.29	0.32	0.36
	Ba^{2+}	0.15	0.19	0.26	0.29	0.33
a_i ($\times 10^{-1}$ mol L^{-1})	Mg^{2+}	1.13	0.67	0.34	0.27	0.20
	Ca^{2+}	0.93	0.56	0.29	0.24	0.18
	Ba^{2+}	0.74	0.47	0.26	0.21	0.16

Table 3
Comparison of effect of the alkaline and alkaline-earth metal cations.

Cation	a (M)	k	C (F g^{-1})	Cation	a (M)	k	C (F g^{-1})		k ratio	C ratio
Li	0.08	−0.21	186.7	Mg	0.10	−0.42	350.1	Mg/Li	2.0	1.9
Na	0.07	−0.34	184.6	Ca	0.09	−0.60	357.9	Ca/Na	1.8	1.9
K	0.07	−0.12	180.7	Ba	0.07	−0.28	298.9	Ba/K	2.3	1.7

The ionic strength, activity coefficient, and cation activity of the electrolytes are shown in Table 2. The capacitances of MnO_2 electrodes on the cation activities are plotted as functions of pLi ($-\log a_{Li}$), pNa ($-\log a_{Na}$), pK ($-\log a_{K}$), pMg ($-\log a_{Mg}$), pCa ($-\log a_{Ca}$), and pBa ($-\log a_{Ba}$). It is previously shown that a linear relationship between capacitance and pLi, pNa, or pK has been obtained [24]. However, it is unknown that whether it fits on alkaline-earth metal cations or not. The linear dependence on pMg, pCa, or pBa is evident as shown in Fig. 4. This linear dependence implies that the charge–discharge process is only determined by insertion–extraction of cations and the charge process is also the first-order reaction with respect to the cation activity of the alkaline-earth metal cations (Mg^{2+}, Ca^{2+}, or Ba^{2+}). The charge rates, k_A, is defined as the slope of the plot of capacitances versus the pA. Therefore k_{Li}, k_{Na}, k_{K}, k_{Mg}, k_{Ca}, and k_{Ba} as listed in Table 3 are −0.21, −0.34, −0.12, −0.42, −0.60, and −0.28, respectively.

3.4. Effect of cation species

In order to discuss the effect of cation species systematically, this section will be divided into three parts. Firstly, we will inves-

tigate the difference among the alkaline metal cations. Secondly, the difference among the alkaline-earth metal cations will be subsequently investigated. Finally, the difference between the alkaline and alkaline-earth metal cations will be addressed.

It can be seen in the previous section that among the alkaline metal cations Na$^+$ ion has the fastest charge rate and largest capacitance have been obtained, while K$^+$ ion represents the opposite. To further discuss the difference among the alkaline metal cations, we have performed the EIS measurements on MnO_2 electrodes in Li_2SO_4, Na_2SO_4 and K_2SO_4 electrolytes with various concentrations ranging from 0.05 to 0.50 M. Fig. 5a and b exhibit the Nyquist plot of MnO_2 electrodes in 0.05 and 0.50 M Li_2SO_4, Na_2SO_4 and K_2SO_4 electrolytes, respectively. All the measured impendence spectra are similar in shape with an arc at higher frequency region and a spike at lower frequency region.

According to Eq. (2), an equivalent circuit shown in Fig. 5a insert can be set up. The model circuit consists of four elements: the internal resistance (R_s), the constant phase element (CPE) used in place of double layer capacitance (C_{dl}), the charge transfer resistance (R_{ct}), and the Warburg impendence (Z_w). The internal resistance
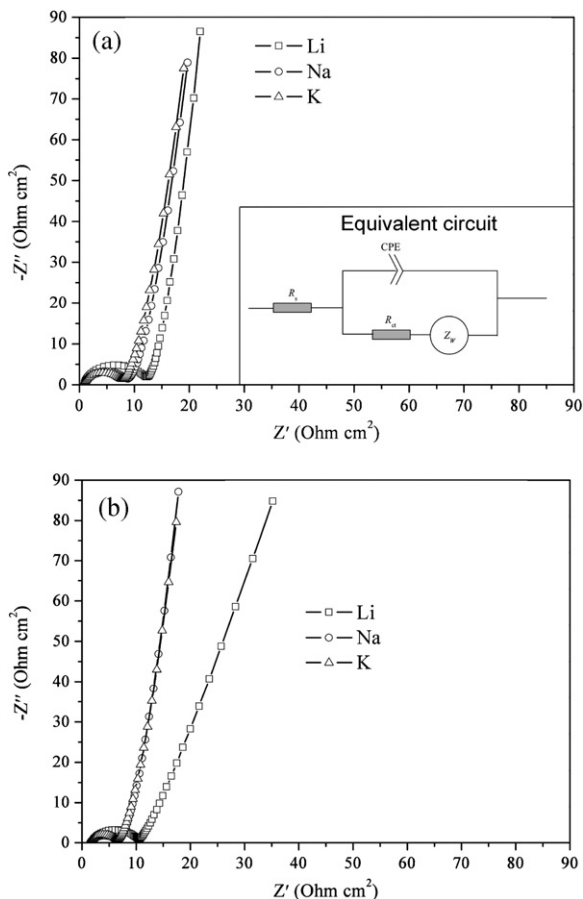

Fig. 5. Nyquist plots of MnO_2 in 0.05 (a) and 0.5 (b) mol L^{-1} Li_2SO_4, Na_2SO_4 and K_2SO_4 electrolytes, respectively. Insert shows the equivalent circuit.
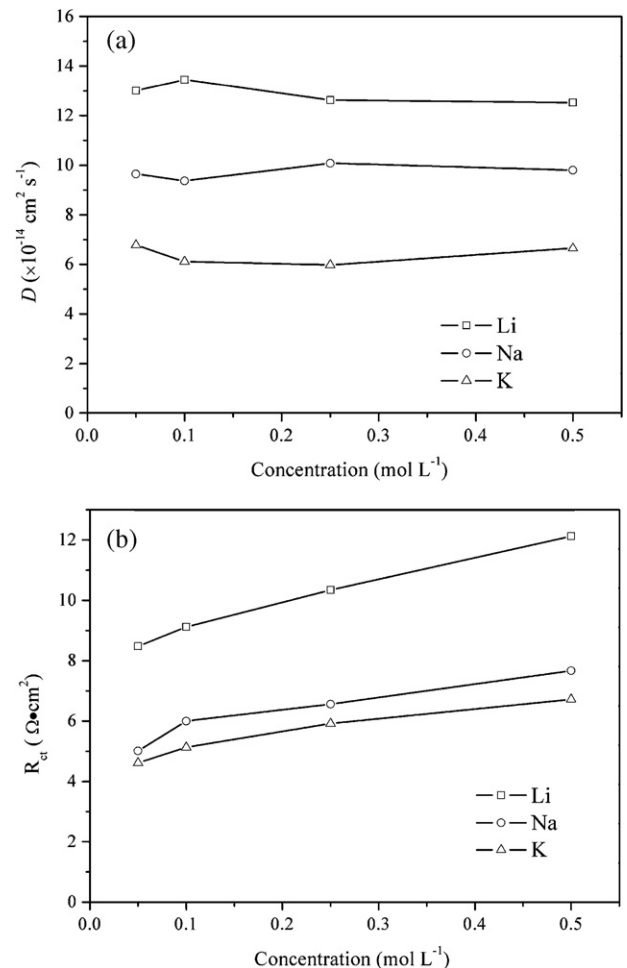

Fig. 6. The fitted diffusion coefficient (a) and R_{ct} (b) for Li_2SO_4, Na_2SO_4 and K_2SO_4 electrolytes with various concentration, respectively.
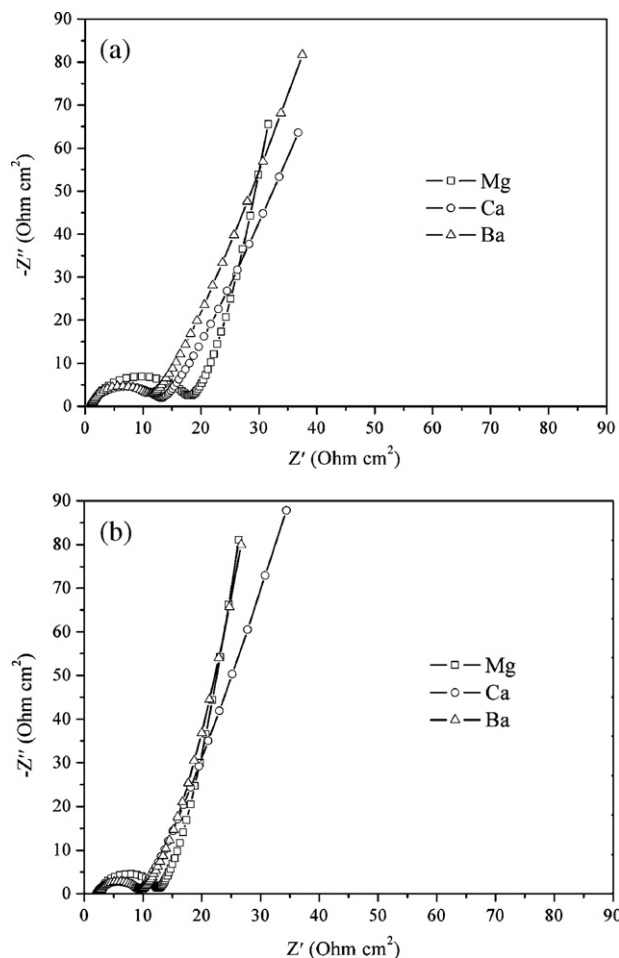
Fig. 7. Nyquist plots of MnO$_2$ in 0.05 (a) and 0.5 (b) mol L^{-1} Mg(NO$_3$)$_2$, Ca(NO$_3$)$_2$ and Ba(NO$_3$)$_2$ electrolytes, respectively.

Fig. 8. The fitted diffusion coefficient (a) and R_{ct} (b) for Mg(NO$_3$)$_2$, Ca(NO$_3$)$_2$ and Ba(NO$_3$)$_2$ electrolytes with various concentration, respectively.

(R_s) includes the bulk electrolyte solution resistance, the intrinsic resistance of active material, and the electron transfer resistance at current collector/electrode boundary. The constant phase element (CPE) is used in place of double layer capacitance (C_{dl}) at the electrode–electrolyte boundary because the non-ideal natures of capacitance arise due to inhomogeneous nature of electrode. The charge transfer resistance (R_{ct}) represents the kinetic resistance to charge transfer at electrode-electrolyte boundary or intrinsic charge transfer resistance of porous electrode. The Warburg impendence (Z_W) associates with the diffusion of cation in the bulk electrode [22,26–28].

Based on the model circuit, the charge process of MnO$_2$ is decided by both the charge transfer resistance (R_{ct}) and the diffusion coefficient (D), which is individually affected by the hydrated ion size and bare ion size of the electrolyte cation. The fitted D and R_{ct} are shown in Fig. 6a and b for Li$_2$SO$_4$, Na$_2$SO$_4$ and K$_2$SO$_4$ electrolytes, respectively. It can be seen from Fig. 6a that the diffusion coefficient is nothing to do with the concentration, but is decided by the ion size. The average D_{Li}, D_{Na} and D_K are 13.3×10^{-14}, 10.6×10^{-14} and 6.8×10^{-14} cm^{-2} s^{-1}, respectively. The smaller bare ion size is, the larger diffusion coefficient is. Fig. 6b exhibits that the larger hydrated ion size is, the larger R_{ct} is.

From the fundamental point of view, the realization of the capacitance of a host material through the redox reaction is determined by the number of intercalated ions concurrent with the charge transfer of the equivalent number of electrons. From a vacancy point of view, the smallest SC value and slowest charge rate for
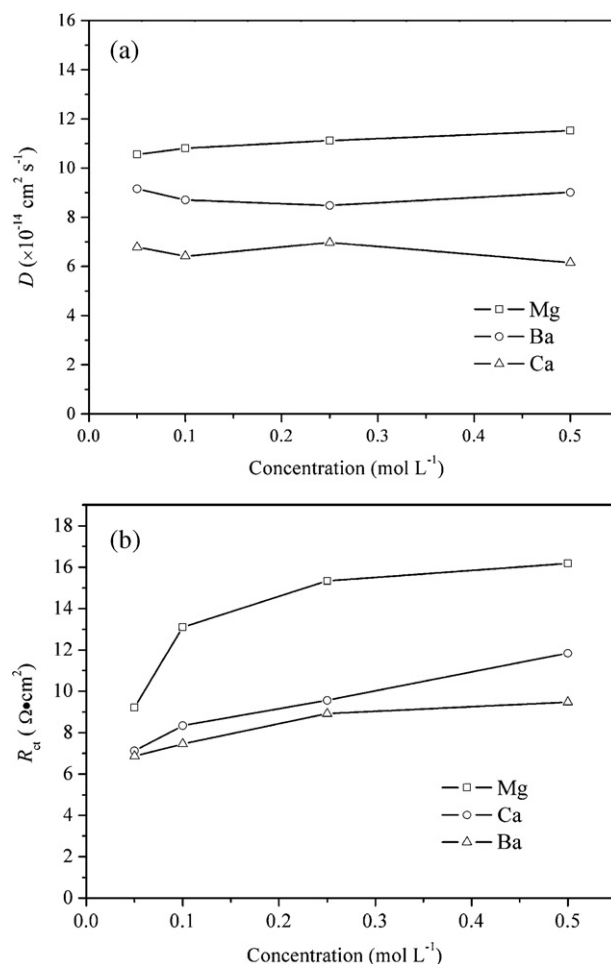
K$^+$ ion are expected, as it is difficult for the K$^+$ with largest ion size to squeeze and diffuse into the MnO$_2$ (smallest D). In the same token, the Li$^+$-cation with the largest hydrated size will encounter highest resistance during the transport in the electrolyte, leading to the slowest charge transfer rate at electrode–electrolyte boundary (largest R_{ct}). With a moderate bare ion size and hydrated size, the Na$^+$ ion may possess moderate diffusion coefficient in MnO$_2$ and mobility in aqueous solution, which seems to be the important factors for the overall large capacitance and fast charge/discharge rate [21].

Among the alkaline-earth metal cations the Ca^{2+} cation has the fastest charge rate and largest capacitance, while Ba^{2+} cation has the opposite. This is in good agreement with the result of the alkaline metal cations. Fig. 7a and b exhibit the Nyquist plots of MnO$_2$ electrodes in Mg(NO$_3$)$_2$, Ca(NO$_3$)$_2$, and Ba(NO$_3$)$_2$ electrolytes of 0.05 and 0.50 M, respectively. All the measured impendence spectra also have the shape with an arc at higher frequency region and a spike at lower frequency region. The results of D and R_{ct} for Mg(NO$_3$)$_2$, Ca(NO$_3$)$_2$, and Ba(NO$_3$)$_2$ electrolytes as determined from the equivalent circuit are shown in Fig. 8a and b, respectively. The average values of D_{Mg}, D_{Ca} and D_{Ba} are 11.0×10^{-14}, 9.2×10^{-14} and 6.4×10^{-14} cm^2 s^{-1}, respectively. These values are of the same order of those for Li$^+$, Na$^+$, and K$^+$ since their ion radius are close as shown in Table 1. The results obtained from the alkaline-earth metal cations are similar to that from the alkaline metal cations, with the largest capacitance value and fastest charge rate for Ca^{2+} cation.

As Li$^+$ and Mg^{2+}, Na$^+$ and Ca^{2+}, and K$^+$ and Ba^{2+}, respectively, have the close ion radius as shown in Table 1, the differences in charging characteristics between each pairs of the alkaline and alkaline-earth metal cations are investigated. As shown in Table 3, the charging rates of the alkaline-earth metal cations are almost the twice of the alkaline metal cations. We reason that one univalent alkaline metal cation intercalated into MnO$_2$ forces one Mn(IV) ion to become Mn(III) ion, while one bivalent alkaline-earth metal cation forces two Mn(IV) ions to become Mn(III) ion. According to the multivalent cation storage mechanism of MnO$_2$, the capacitance has to be doubled by using the bivalent alkaline-earth metal cations to replace the alkaline metal cations. We firstly compare the alkaline metal cations with the alkaline-earth metal cations at the same cation concentration. The capacitance of MnO$_2$ in 0.25 M Li$_2$SO$_4$, Na$_2$SO$_4$, and K$_2$SO$_4$ electrolytes are 200.6, 221.2, and 189.8 F g^{-1}, and in 0.5 M Mg(NO$_3$)$_2$, Ca(NO$_3$)$_2$, and Ba(NO$_3$)$_2$ electrolytes are 350.1, 357.9, and 298.9 F g^{-1}, respectively. The capacitance ratio of Mg/Li, Ca/Na, and Ba/K are only 1.7, 1.6 and 1.6, respectively. However, if taking account of the effect at a close cation activity shown in Table 2, for instance, 0.5 M for the alkaline-earth metal cations concentration and 0.1 M for the alkaline metal cations concentration, the capacitance ratio of Mg/Li, Ca/Na, and Ba/K are 1.9, 1.9 and 1.7, respectively, as listed in Table 3. The results clearly confirm the function of the multivalent cation storage mechanism of MnO$_2$. In addition, in order to compare the electrochemical behavior of MnO$_2$ among the various electrolytes, the cation activity of the electrolyte instead of the salt concentration has to be selected closely.

4. Conclusion

The effect of the electrolyte particularities on manganese dioxide in the neutral electrolytes for electrochemical capacitor has been investigated by cyclic voltammetry and electrochemical impedance spectroscopy. The results show that cations of the electrolyte instead of proton or anions are responsible for the pseudo-capacitive behavior of manganese dioxide. The capacitance of manganese dioxide was found to depend strongly on the electrolyte particularities, for example, pH value, cation species and concentrations. A logarithmic dependence of capacitance of MnO$_2$ on cation activity has been obtained for all alkaline and alkaline-earth metal cations. The capacitance of MnO$_2$ has been doubled by replacing univalent cation with bivalent cation at a close cation activity and bare ion size.

References

[1] B.E. Conway, Electrochemical Supercapacitor: Scientific Fundamentals and Technological Applications, Kluwer Academic/Plenum Publishers, New York, 1999.
[2] A. Burke, J. Power Sources 91 (2000) 37.
[3] H.Y. Lee, J.B. Goodenough, J. Solid State Chem. 148 (1999) 81.
[4] C. Xu, F. Kang, B. Li, H. Du, J. Mater. Res. 25 (2010) 1421.
[5] H.Y. Lee, J.B. Goodenough, J. Solid State Chem. 144 (1999) 220.
[6] T. Brousse, P.-L. Taberna, O. Crosnier, R. Dugas, P. Guillemet, Y. Scudeller, Y. Zhou, F. Favier, D. Bélanger, P. Simon, J. Power Sources 173 (2007) 633.
[7] C. Xu, B. Li, H. Du, F. Kang, Y. Zeng, J. Electrochem. Soc. 156 (2009) A435.
[8] M. Ghaemi, F. Ataherian, A. Zolfaghari, S.M. Jafari, Electrochim. Acta 53 (2008) 4607.
[9] M. Toupin, T. Brousse, D. Bélanger, Chem. Mater. 16 (2004) 3184.
[10] L. Athouel, F. Moser, R. Dugas, O. Crosnier, D. Bélanger, T. Brousse, J. Phys. Chem. C 112 (2008) 7270.
[11] C.-C. Hu, Y.-T. Wu, K.-H. Chang, Chem. Mater. 20 (2008) 2890.
[12] C.-C. Hu, Y.-T. Wu, Electrochem. Commun. 4 (2002) 105.
[13] S.-C. Pang, M.A. Anderson, T.W. Chapman, J. Electrochem. Soc. 147 (2000) 444.
[14] J.-K. Chang, M.-T. Lee, W.-T. Tsai, M.-J. Deng, I.-W. Sun, Chem. Mater. 21 (2009) 2688.
[15] M.-T. Lee, W.-T. Tsai, M.-J. Deng, H.-F. Cheng, I.-W. Sun, J.-K. Chang, J. Power Sources 195 (2010) 919.
[16] K.-W. Nam, M.G. Kim, K.-B. Kim, J. Phys. Chem. C 111 (2007) 749.
[17] O. Ghodbane, J.-L. Pascal, F. Favier, Appl. Mater. Inter. 1 (2009) 1130.
[18] T. Brousse, M. Toupin, R. Dugas, D. Bélanger, J. Electrochem. Soc. 153 (12) (2006) A2171.
[19] S. Devaraj, N. Munichandraiah, J. Phys. Chem. C 112 (2008) 4406.
[20] S. Wen, J.-W. Lee, I.-H. Yeo, J. Park, S.-I. Mho, Electrochim. Acta 50 (2004) 849.
[21] C. Xu, B. Li, H. Du, F. Kang, Y. Zeng, J. Power Sources 184 (2008) 691.
[22] C. Xu, B. Li, H. Du, F. Kang, Y. Zeng, J. Electrochem. Soc. 156 (1) (2009) A73.
[23] J.A. Dean, Lange's Handbook of Chemistry, McGraw Hill, 1992.
[24] C. Xu, B. Li, H. Du, F. Kang, Y. Zeng, J. Power Sources 180 (2008) 664.
[25] A. Zolfaghari, F. Ataherian, M. Ghaemi, A. Gholami, Electrochim. Acta 52 (2007) 2904.
[26] S. Devaraj, N.J. Munichandraiah, J. Electrochem. Soc. 154 (2007) A901.
[27] R. Kötz, M. Carlen, Electrochim. Acta 45 (2000) 2487.
[28] J. Rishpon, S. Gottesfield, J. Electrochem. Soc. 131 (1984) 1960.